Structure and Catalytic Properties of Magnesia-Supported Copper Salts of Molybdovanadophosphoric Acid

Guangdong Zhou,[†,‡] Xiaomei Yang,[†] Jie Liu,[†] Kaiji Zhen,[†] Haishui Wang,*[,‡] and Tiexin Cheng*[,†]

College of Chemistry, Jilin University, Changchun 130021, China, and Changchun Institute of Applied Chemistry, Chinese Academy of Sciences, Changchun 130022, China

Received: January 13, 2006; In Final Form: April 1, 2006

The structure and stability of magnesia-supported copper salts of molybdovanadophosphoric acid ($Cu_2PMo_{11}VO_{40}$) were characterized by different techniques. The catalyst was prepared in ethanol by impregnation because this solvent does not hurt texture of the water-sensitive MgO and $Cu_2PMo_{11}VO_{40}$. The Keggin-type structure compound may be degraded partially to form oligomerized polyoxometalate when supported on MgO. However, the oligomers can rebuild as the Keggin structure again after thermal treatment in air or during the reaction. Meanwhile, the V atoms migrate out of the Keggin structure to form a lacunary structure, as observed by Fourier transform IR spectroscopy. Moreover, the presence of Cu^{2+} as a countercation showed an affirmative influence on the migration of V atoms, and the active sites derived from the lacunary species generated after release of V from the Keggin anion. The electron paramagnetic resonance data imply that V^{5+} autoreduces to V^{4+} in the fresh catalyst, and during the catalytic reaction a large number of V^{4+} ions are produced, which enhance the formation of O^{2-} vacancies around the metal atoms. These oxygen vacancies may also improve the reoxidation function of the catalyst. This behavior is correlated to higher catalytic properties of this catalyst. The oxidative dehydrogenation of hexanol to hexanal was studied over this catalyst. After reaction at 553.2 K for 50 h, catalytic properties did not decrease and exhibited higher selectivity (>96.0%) toward hexanal.

1. Introduction

Heteropolyacids (HPA) and their salts are useful commercial catalysts for acid as well as oxidation catalysis.[1,2] They are highly effective heterogeneous catalysts for the gas-phase selective oxidation of organic substrates.[3,4]

The HPAs with Keggin-type structure possess special characteristics that make them very active in catalytic reaction. Good reoxidativity of the catalyst by air and mobility of lattice oxygen are necessary for high activity. 12-Molybdophosphoric heteropolyacid (PM), in which vanadium atoms substitute a part of molybdenum atoms, has been found as an effective catalyst. Theoretically, the vanadium atoms in the Keggin unit contribute to the reduction of the acid strength and to the enhancement of the reoxidativity.[1,5−8]

As a rule, differences of this type of catalysts depend on whether the counterions are transition-metal ions, alkali metal, or alkaline earth metal ions. Indeed, the transition metal cations may circulate their valence states in catalytic oxidation reaction[9,10] and then may stabilize the catalytic system unlike the other two types of ions. As reported in refs 11−13, copper is an attractive counterion of the Keggin unit $PMo_{11}VO_{40}^{4-}$.

A disadvantage of HPAs as catalysts lies in their low stability and surface area, caused by various factors. In molybdophosphoric acid, thermal decomposition, acidity changes, and loss of the active phase occur, which are due to formation of volatile molybdic acid.[14] To overcome this disadvantage, the HPA may be supported on different carriers[8] by using impregnating solution in different solvents,[15] but different results have been published.[16−24]

The oxidation of alcohols into aldehydes and ketones is a ubiquitous transformation in organic chemistry, and numerous oxidizing agents and noble metals are available to effect this key reaction.[25−27] However, the noble metals are not only relatively expensive but also generate copious amounts of heavy-metal waste. Moreover, the reactions are often performed in environmentally undesirable solvents, typically chlorinated hydrocarbons, which are hazardous and the overgrowing environmental concern.

In the present paper, we report the MgO-supported copper salts of molybdovanadophosphoric acid ($Cu_2PMo_{11}VO_{40}$, noted as CPMV) for partial oxidation of hexanol to hexanal.

2. Experimental Section

2.1. Catalyst Preparation. HPA $H_4PMo_{11}VO_{40}$ was prepared according to the method of Tsigdions.[28] The copper salt of HPA $Cu_2PMo_{11}VO_{40}$ was synthesized by addition of a stoichiometric amount (2:1 mol ratio) of $Cu_2(OH)_2CO_3$ to an ethanol solution of $H_4PMo_{11}VO_{40}$ and then drying at room temperature.

A two-step method was used to prepare MgO-supported heteropoly compounds.[29] The copper source was previously deposited on the MgO support surface (E. Merck, Brunauer−Emmett−Teller (BET) surface area: 110 m^2/g, calcined at 673.2 K for 2 h) by impregnation from an ethanol solution of the corresponding cupric nitrate. After drying at 393.2 K for 12 h, the samples were calcined in air at 773.2 K for 2 h. The Keggin anion was brought in by impregnation from an ethanol solution of the molybdovanadophosphoric acid ($H_4PMo_{11}VO_{40}$, noted as PMV), followed by drying at 373.2 K for 2 h and at 393.2

* Corresponding authors. Phone, +86-431-8499356 (C.T.), +86-431-5262054 (W.H.); E-mail, ctx@jlu.edu.cn (C.T.), hswang@ciac.jl.cn (W.H.).
† Jilin University.
‡ Chinese Academy of Sciences.

10.1021/jp060241e CCC: $33.50
Published on Web 05/02/2006

K for 12 h. The concentration and the volume of the impregnating solutions were adjusted to ensure a Cu^{2+} to $PMo_{11}VO_{40}^{4-}$ ratio of 2. The amount of CPMV deposited on the MgO surface was 13.0, 23.1, and 31.0 wt. %, respectively (noticed as CPMV/MgO). For comparison, the supported catalyst was also synthesized by impregnation in an ethanol solution of the $Cu_2PMo_{11}VO_{40}$ and the first step was performed with only MgO in the ethanol. The amount of the loaded CPMV in the catalyst was 23.1 wt. %, which is noticed as $CPMV/MgO_{comparison}$.

2.2. Catalyst Characterizations. A Nicolet-Impact 400 Fourier-transformed infrared (FTIR) spectrometer was employed to test the vibrational behavior of the sample containing KBr and a range of ~400−1500 cm^{-1} was scanned. The X-ray diffraction (XRD) patterns were obtained using a Shimadzu XRD-6000 diffractometer with CuKα radiation (0.15406 nm), nickel filter, angle range (2θ) from 3 to 80°, and at a scanning rate of 4°/min. The BET surface area was measured on a Micrometitics ASAP-2010 using nitrogen at liquid nitrogen temperature. MAS NMR measurement of the samples was carried out on an Infinity Plus-400 equipment, using 15-μs pulses, a repetition time of 60 s, and working at a frequency of 161.87899 MHz at room temperature. Chemical shifts of ^{31}P were referenced to external calibration using 85% phosphoric acid. The spinning rate was 7.0 kHz, and 90 responses were collected. Thermogravimetric analysis (TGA) and differential thermal analysis (DTA) were performed using a Netzscn STA 449C thermogravimetric analyzer. Samples were heated in air from 303.2 to 873.2 K at a rate of 20 K/min. The electron paramagnetic resonance (EPR) spectra were recorded on a Bruker ER 200D at X-band frequency at 77 K, microwave frequency about 9.68 GHz, microwave power 20.5 mW, and modulation frequency 100 kHz. The g values were determined with DPPH as g marker.

2.3. Catalytic Activity. The reaction was carried out in a fixed-bed continuous-flow quartz reactor operated under atmospheric pressure. In each run, 0.4 cm^3 catalyst was placed in the center of the reactor and fixed by quartz glass wool plugs. Hexanol was fed (0.015 mol/h) to the reactor by passing highly pure nitrogen (54 cm^3/min) and oxygen 6 cm^3/min (0.015 mol/h). Before reaction the catalyst was heated at 373.2 K for 30 min, 473.2 K for 30 min, and at 623.2 K for 1 h in highly pure nitrogen, respectively. Reaction products were analyzed using a Shimadzu GC 14B gas chromatograph equipped with a fused silica capillary column and a flame ionization detector (FID).

3. Results and Discussion

3.1. DTA-TGA Results. The DTA-TGA profile of MgO is shown Figure 1. Basically, two groups of peak can be observed: as usually an endothermic peak is at 405.2 K, while at higher temperatures (636.3 and 665.9 K) two more overlap endothermic peaks appear. The first endothermic peak belongs to the loss of adsorbed water from the surface of MgO. The two overlap endothermic peaks belong to the loss of hydroxyl groups, which shows that two types of hydroxyl groups, i.e., hydration and free hydroxyl groups are dispersed on the surface of MgO.[30]

The thermal stability of the bulk PMV and CPMV were also investigated by means of DTA-TGA (Figures 2 and 3). The TGA profile of the PMV shows a weight loss in two steps, which are due to the removal of crystalline water and constitutional water, respectively. The amounts of crystalline water (8 mol) and of constitutional water (1.8 mol) agree approximately with the nominal stoichiometry indicating the chemical formula of the sample ($H_4PMo_{11}VO_{40}\cdot 8H_2O$). The

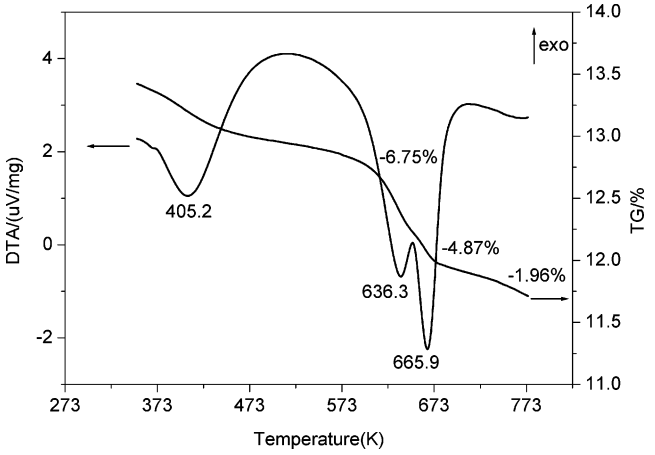

Figure 1. DTA-TGA profile of MgO.

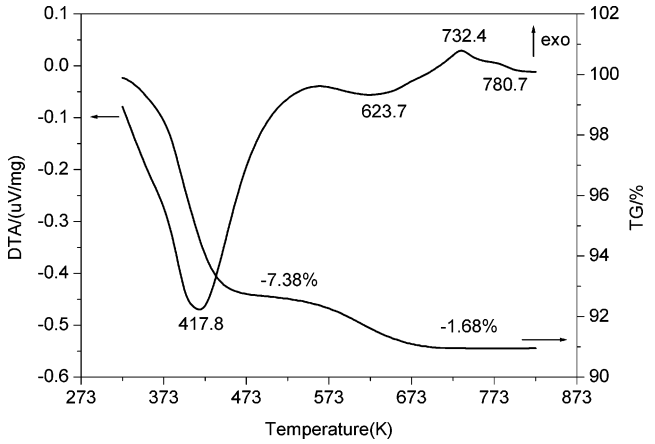

Figure 2. DTA-TGA profile of $H_4PMo_{11}VO_{40}$.

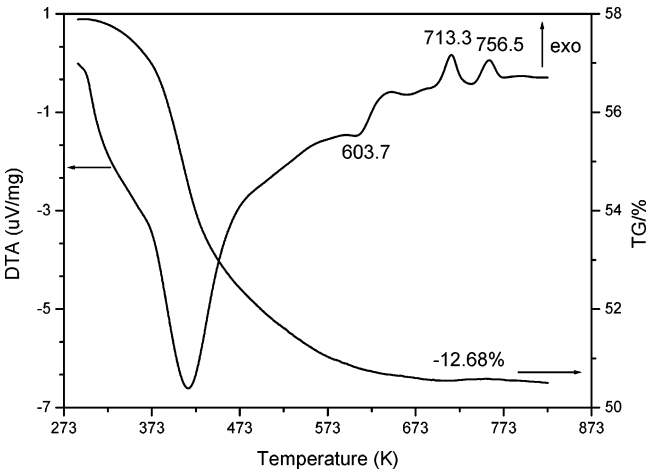

Figure 3. DTA-TGA profile of $Cu_2PMo_{11}VO_{40}$.

DTA profile of the PMV also shows two endothermic peaks, which correspond to water loss at 417.8 and 623.7 K, respectively. The decomposition of the bulk PMV is verified by an exothermic peak at around 732.4 K, which is associated with the decomposition of PMV to corresponding oxides. A small exothermic peak at 780.7 K is due to exothermic crystallization of the oxides.

The two types of endothermic peaks responsible for the loss of water are also observed for CPMV. J. Haber has reported[31] that the area of these peaks was strictly related with the number of cations incorporated. The first peak observed at about 414.6 K, related to the removal of the crystalline water, is independent

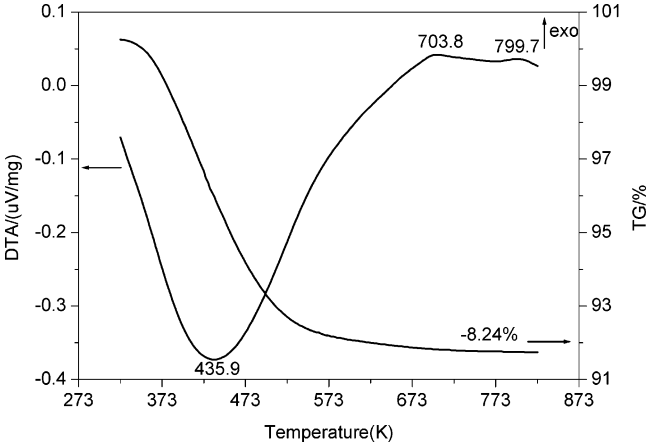

Figure 4. DTA-TGA profile of $Cu_2PMo_{11}VO_{40}$/MgO.

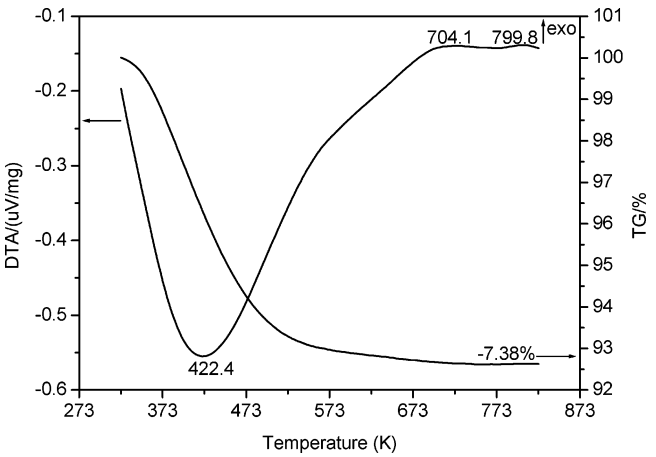

Figure 5. DTA-TGA profile of $Cu_2PMo_{11}VO_{40}$/$MgO_{comparison}$.

of the number of cations contained; the second one (603.7 K) originates from the loss of the constitutional water, which decreases with the increase in the cation content in HPAs. For the copper salt, this type of peak being smaller indicates that $Cu_2PMo_{11}VO_{40}$ has formed incompletely or appears another kind of water, which coordinates cation in the Keggin structure.[31] The complete decomposition of CPMV with the formation of oxides corresponds to the large exothermic effect at 713.3 K, another exothermic peak at 756.5 K results from exothermic crystallization of oxides.

In the case of supported catalyst (Figure 4), an endothermic peak is observed at about 435.9 K, but the endothermic peak due to loss of constitutional water cannot be obtained. The two reasons were supposed: one of them is that a full salt $Cu_2PMo_{11}VO_{40}$ was formed on the surface support; the other one is that the intensity of peak becomes weaker for the supported catalyst. This seems to confirm that monophase of the $Cu_2PMo_{11}VO_{40}$ salt has formed on the surface of MgO. In addition, two smaller exothermic peaks are observed for this sample at 703.9 and 799.7 K, respectively, which suggest that decomposition of some CPMV and exothermic crystallization of the formed oxides take place. Thermal analyses confirm that there exists a strong interaction between the Keggin anion and the MgO support, which results in an increase of temperatures of decomposition and exothermic crystallization, respectively.

To prove if copper salt of $H_4PMo_{11}VO_{40}$ is formed on the surface of MgO, the DTA-TGA profile of the CPMV/$MgO_{comparison}$ sample is shown in Figure 5. We found that both CPMV/MgO and CPMV/$MgO_{comparison}$ showed quite similar thermograms. This indicated that the samples prepared by

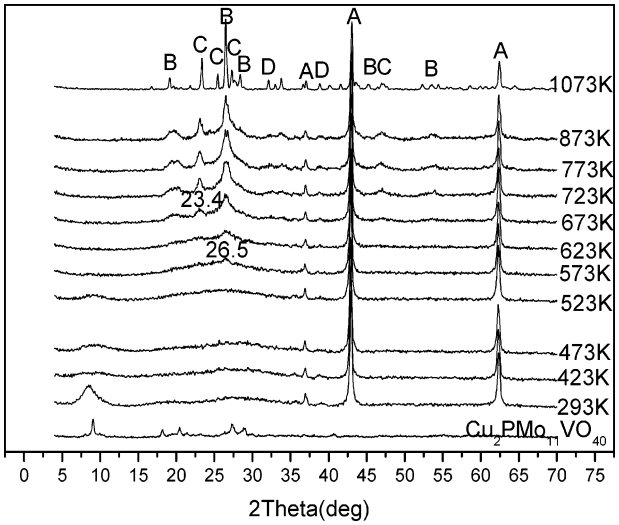

Figure 6. XRD spectra of catalysts as-synthesized and calcined at different temperatures for 2 h: (A) MgO; (B) V_2O_5; (C) MoO_3; (D) CuO.

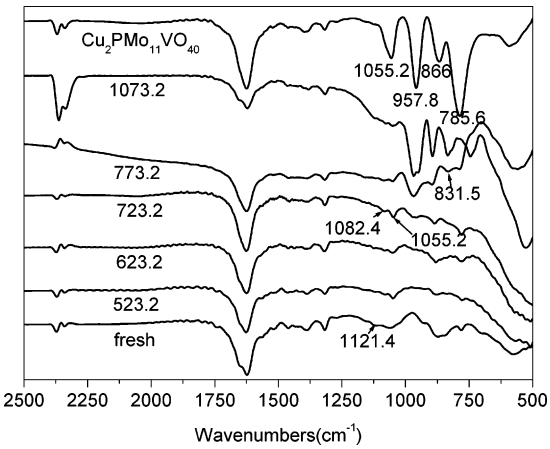

Figure 7. IR spectra of the MgO-supported catalysts treated at different temperatures.

different impregnation methods possessed the same characteristics on the structures; i.e., the copper salt of $H_4PMo_{11}VO_{40}$ was formed by the two-step preparation recipe.

3.2. XRD Results. Figure 6 shows X-ray diffractograms of $Cu_2PMo_{11}VO_{40}$, as-synthesized and calcined at different temperatures. Some intense peaks are shown for the CPMV sample in a range of 8−30°, i.e., 8.9, 18.1, 20.4, 27.4, and 28.9°, which are attributed to characteristic diffraction of Keggin anion.

The fresh-supported catalyst also shows diffraction peaks of CPMV. Three intense signals at 37.1, 43.0, and 62.4°, assigned to MgO are observed for samples calcined in a temperature range of 393.2−1073.2 K. These diffraction peaks of CPMV gradually disappear with increasing calcination temperature and a new peak at 26.5° appears for the sample calcined in a temperature range of 573.2−1073.2 K, which is assigned to a new phase of vanadium−oxygen cluster. It has been proposed that a part of vanadium atoms could expel from the Keggin structure CPMV under thermal treatment and form a new phase, which is assigned to $[(VO)(PMo_{11}O_{39})]^{4-}$. The IR spectra (Figure 7) of the samples calcined at 773.2 K show a V_2O_5 characteristic peak at 831.5 cm^{-1}, suggesting that this lacunary structure is stable up to 773.2 K. In fact, the other XRD peaks of the samples calcined below 873.2 K cannot be simply attributed to pure oxides. However, at 1073.2 K the Keggin type CPMV can completely decompose to corresponding oxides.

3.3. FTIR Results. The $Cu_2PMo_{11}VO_{40}$ shows four characteristic peaks (Figure 7) in the region ~1100−400 cm^{-1}, i.e., 1055.2, 957.8, 866, and 785.6 cm^{-1}, which are assigned to the stretching vibrations of P−O_a, Mo═O_d, Mo−O_b−Mo and Mo−O_c−Mo, respectively. Previous work[32] shows that the substituting transition metal induces a decrease of the oxoanion symmetry, leading to split of the asymmetric (P−O_a) stretching vibration. As a consequence, the shoulder peak does not appear in the (P−O_a) band for the CPMV. In addition, the vibration of V−O band cannot be seen probably because of the very strong absorption of Mo═O band.[33]

Supporting CPMV on MgO results in lowering the intensities of characteristic IR vibrations of CPMV and changed in their positions. Figure 7 shows the spectra of 23.1 wt. % $Cu_2PMo_{11}VO_{40}$/MgO calcined at different temperatures. The spectrum of the fresh catalyst exhibits two broad and weak bands at 1121.4 and 1055.2 cm^{-1}, which are attributed to adsorbed carbon species on the MgO surface and P−O band, respectively. It is shown that the carbon species band disappears with increase in the calcination temperature to 523.2 K. In contrary, a new absorption peak at 1082.4 cm^{-1} appears, the intensity of which should be highlighted when heated to 723.2 K. Simultaneously, the four characteristic bands of Keggin-type structure also become more pronounced after calcined at higher temperature (≤723.2 K). This proves that the Keggin structure is in a higher symmetric environment after thermal treatment, i.e., for the fresh catalyst, though the Keggin-type structure has partially degraded to formed lower symmetric oligomers, which can restore to the higher symmetric polyanions of $PMo_{11}VO_{40}^{4-}$ again.

As described in the previous section, for the unsupported CPMV, no split of antisymmetric P−O_a vibration corresponding to lowering symmetry of the central PO_4 tetrahedron was obtained. However, for the supported catalyst, a new shoulder peak (i.e., splitting peak) appears at 1082.4 cm^{-1}, which is inferred that a few V atoms have already located outside the Keggin anion of the fresh catalyst. As the temperature increases the V ions gradually remove from the Keggin unit and result in the formation of lacunar heteropoly anion

$$[PMo_{11}VO_{40}]^{4-} \rightarrow [VO]^{3+}[PMo_{11}O_{39}]^{7-}$$

For the $Cu_2PMo_{11}VO_{40}$/MgO sample calcined at 773.2 K, a new peak is observed at 831.5 cm^{-1}, which is assigned to characteristic vibration of V_2O_5.[34] This proves degradation of the Keggin unit at 773.2 K. With heating to 1073.2 K, the Keggin unit completely decomposes to correspondent oxides.

For the sample calcined at 723.2 K for 2 h and then stored at room temperature for one week in air, the splitting peak disappears (Figure 8), indicating that V ions return into the Keggin anion, or the highly unstable $PMo_{11}O_{39}^{7-}$ lacunary species transforms to $PMo_{12}O_{40}^{3-}$.[35]

Figure 9 shows the FTIR spectra of $Cu_2PMo_{11}VO_{40}$/MgO after the catalytic reaction at 553.2 K for different periods of time. After 10 h of reaction, the spectrum shows apparently superposition of two signals (Figure 9b) at 1082.4 and 1055.2 cm^{-1}. The first is characteristic of a splitting P−O band, and the second is ascribed to the P−O_a band, which verifies that a small amount of V ions already removed from the Keggin anion. After 50 h of reaction, the intensity of the peak at 1082.4 cm^{-1} increases, confirming that a large amount of V ions remains outside the Keggin unit. This fact proves formation of a lacunary structure of the catalyst during the reaction.

On the other hand, comparing the IR spectra of $Cu_2PMo_{11}VO_{40}$/MgO after reaction at 553.2 for 50 h and $Cu_2PMo_{11}VO_{40}$/$MgO_{comparion}$, it can be found that both samples show very similar IR characteristic vibrations. This phenomenon confirms that the $Cu_2PMo_{11}VO_{40}$ can keeps its Keggin-type structure, and the supported salt of the heteropoly acid may be prepared by the two step impregnation method.

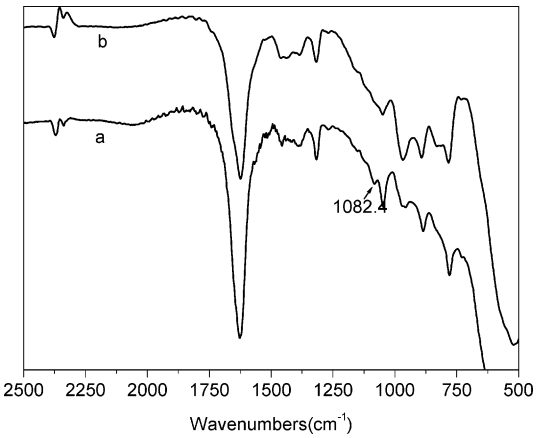

Figure 8. IR spectra of $Cu_2PMo_{11}VO_{40}$/MgO calcined at 723.2 K in air for 2 h (a) and stored at room temperature in air for one week (b).

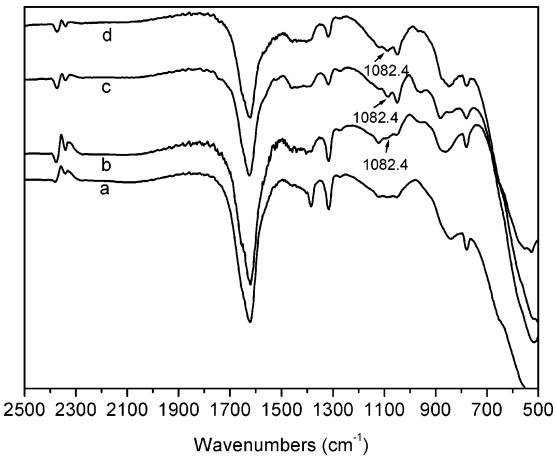

Figure 9. IR spectra of the different samples. Freshly synthesized (a), $Cu_2PMo_{11}VO_{40}$/MgO after reaction at 553.2 K for 10 h (b), 50 h (c) and $Cu_2PMo_{11}VO_{40}$/$MgO_{comparison}$ (d).

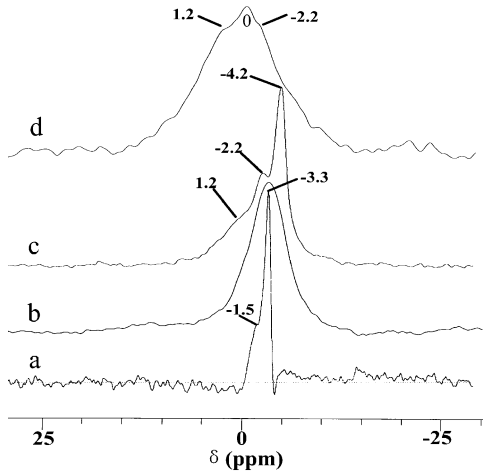

Figure 10. ^{31}P NMR spectra of $H_4PMo_{11}VO_{40}$ (a), $Cu_2PMo_{11}VO_{40}$ (b), fresh $Cu_2PMo_{11}VO_{40}$/MgO (c), and $Cu_2PMo_{11}VO_{40}$/MgO after calcination at 723.2 K for 2 h (d).

3.4. NMR Results. Figure 10 displays the ^{31}P MAS NMR spectra of $H_4PMo_{11}VO_{40}$, $Cu_2PMo_{11}VO_{40}$, $Cu_2PMo_{11}VO_{40}$/MgO, and $Cu_2PMo_{11}VO_{40}$/MgO after thermal treated at 723.2 K for 2 h. The solid state ^{31}P MAS NMR spectrum of the

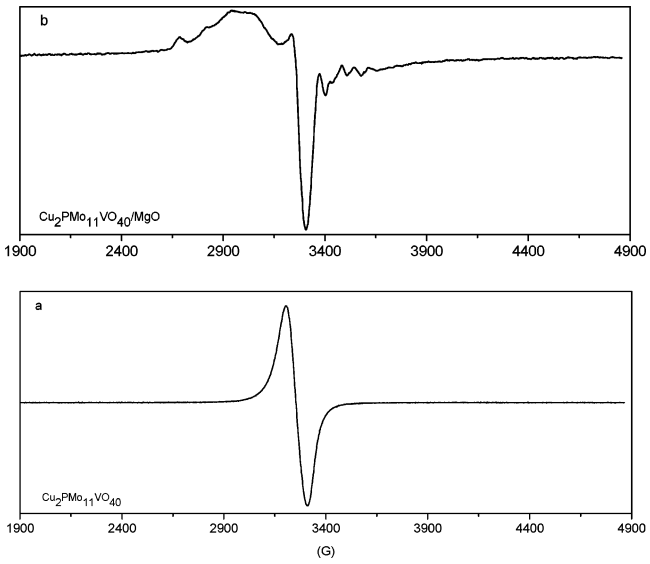

Figure 11. EPR spectra of $Cu_2PMo_{11}VO_{40}$ (a) and $Cu_2PMo_{11}VO_{40}$/MgO (b).

hydrated PMV (Figure 10a) shows a strong resonance peak at −3.3 ppm, which is characteristic of the Keggin structure of HPA and a small shoulder at −1.5 ppm, which results from change in the circumstance of phosphorus atom due to a small difference in the degree of hydration.[31] As shown in Figure 10b, only a broad peak at −3.3 ppm exists for the CPMV. A. G. Siahkali[36] proposes that the peak width differences in ^{31}P spectra are related to the removal of crystalline water and structural water, respectively. As shown in Figure 10c in the ^{31}P-MAS NMR spectrum of $Cu_2PMo_{11}VO_{40}$/MgO containning 23.1 wt. % CPMV appear three resonance peaks. The first one at −4.2 ppm is sharp and is contributed to the CPMV with Keggin structure, and the small upfield shift can be attributed to the heteropolyanion in slight interaction with the support surface. The second one at −2.2 ppm is a shoulder peak, which could be assigned to a lacunary form of the CPMV resulted from its interaction with the supporting material. Because of the extreme sensitivity of ^{31}P nucleus to its local environment, any slight change in the chemical environment due to the interaction between the support and CPMV could cause the difference.[37] The third one at 1.2 ppm is much broader and cannot be completely assigned. It may happen that the heteropolyanions are in stronger interaction with the surface, which results in a distorted form of the heterpolyanion or phosphate formed from decomposition of heteropolyanion. On the other hand, Kasztelan[38] and Mastikhin[39] concluded that three types of HPA are present on the support surface depending on the concentration of HPA: isolated or highly dispersed surface HPA at low concentration, then aggregates or clusters are formed, and at high loadings crystals or particles of HPA are present. In these cases the changes of ^{31}P chemical shift are different. The spectrum of the calcined catalyst is given in Figure 10d. A much broader line with a maximum at 0 ppm was observed, although the signal enlargement can be attributed to an intense interaction then thermal treatment. These obtained results prove that the CPMV on the MgO support can keep the Keggin structure, although partial decomposition of it may appear.

3.5. EPR Results. Parts a and b of Figure 11 show EPR spectra measured at 77 K for $Cu_2PMo_{11}VO_{40}$ and $Cu_2PMo_{11}VO_{40}$/MgO, respectively. Apparently, a normal paramagnetic signal at $g = 2.165$ with an axial symmetry can be ascribed to Cu^{2+} ions. The signal of the paramagnetic copper (II) center could also be observed for the supported catalyst $Cu_2PMo_{11}VO_{40}$/MgO and shows a low-field hyperfine structure also ascribed to the Cu^{2+} ion. This phenomenon may be caused by dispersion of the CPMV on the support surface and/or migration of vanadium atoms out of the Keggin anion leading to that the Cu^{2+} ions of the supported catalyst are surrounded by more ligands. The increase in copper coordination number results in larger $Cu^{2+}-O^{2-}$ length. However, for the pure CPMV the hyperfine structure cannot be surveyed, due to agglomeration of Cu^{2+} in case of higher copper contents in the compound which leads to a strong dipolar interaction between the copper (II) ions arising from the shortening of the Cu−O bond length.

TABLE 1: Catalytic Properties of the Different Samples at 553.2 K[a]

	conv. %	yield (%)			selec (%)		
catalysts	hexanol	hexene	pentanal	hexanal	hexene	pentanal	hexanal
a	18.7	0	0	18.7	0	0	100
b	36.8	0.5	0	36.3	1.4	0	98.6
c	21.4	0.6	0	20.8	2.8	0	97.2
d	33.5	0	0.7	32.8	0	2.1	97.9
e	11.4	0.4	0	11.0	3.7	0	96.3
f	8.2	0	0	8.2	0	0	100
g	7.2	1.4	0	5.8	19.4	0	80.6

[a] The different $Cu_2PMo_{11}VO_{40}$ content in the CPMV/MgO: (a) 13.0%, (b) 23.1%, (c) 31.0%, (d) 23.1% (CPMV/$MgO_{comparison}$), (e) after calcination at 1073 K for 2 h, (f) MgO, (g) $Cu_2PMo_{11}VO_{40}$. Hexanol, 0.015 mol/h; oxygen, 6 mL/min; GHSV, 9000 h^{-1}.

The magnetic field lines observed on the right-hand side of Cu^{2+} signal can be assigned to a vanadyl species outside the Keggin unit as a counterion to Keggin unit in the secondary structure.[40] From the EPR experiment results, it can be proposed that the vanadium ions substitute molybdenum ions in the Keggin unit. These substituting vanadium ions are ejected from Keggin unit on the supported catalyst and underwent autoreduction to V^{4+}. J. K. Lee[40] considered that the reduction of the central transition metal atoms (V, Mo) would be explained by the oxidation of O^{2-} ligands (lattice oxygen) to molecular O_2, which transfer to atmosphere (also called autoreduction), and the degree of reduction depends strongly on the type of counterion, treatment temperature, and atmosphere. E. Blowel-Crusson[41] suggested that the counterion accelerates the interaction between V^{5+} ions and mobile electrons; thus, the autoreduction and removal of the V ions from the Keggin unit are also improved. Meanwhile, the copper atoms seem to enhance the formation of O^{2-} vacancies surrounding the vanadium atoms and can improve the mobility of lattice oxygen necessary for a good oxidation catalyst.

3.6. Catalytic Properties. The catalytic properties of the different samples at 553.2 K are listed in Table 1, it shows that the catalyst containing 23.1 wt. % CPMV is the most active for conversion of hexanol to hexanal. Moreover, the properties are close for the CPMV/MgO and CPMV/$MgO_{comparison}$ (23.1 wt. % CPMV), suggesting that the same species are present on the MgO surface no matter which the preparation procedure is used. The samples after thermal treatment at 1073.2 K for 2 h show lower catalytic activity than other supported catalysts, because the CPMV on the surface of MgO has decomposed to corresponding oxides. In addition, it is also observed that the MgO and bulk $Cu_2PMo_{11}VO_{40}$ show the lowest activity too.

Figure 12 displays the variation of the conversion and selectivity in the oxidative dehydrogenation of hexanol over the $Cu_2PMo_{11}VO_{40}$/MgO catalyst at different temperatures. The hexanol conversion reaches 44.2% at 593.2 K, and a hexanal selectivity of 100% is obtained at 513.2 and 533.2 K. A maximum yield of hexanal (41.4%) is obtained at 593.2 K at a

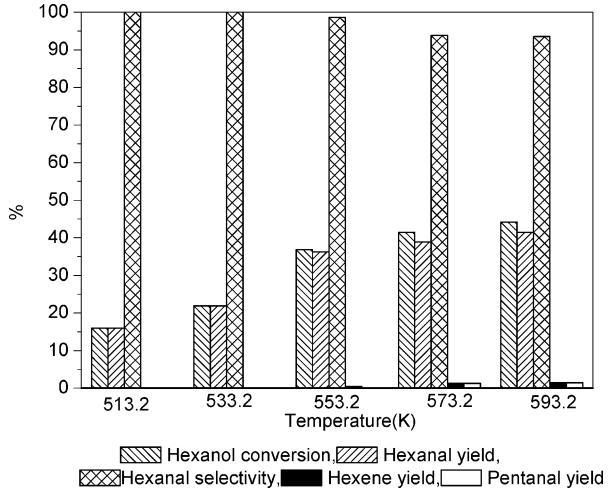

Figure 12. Catalytic properties of $Cu_2PMo_{11}VO_{40}$/MgO.

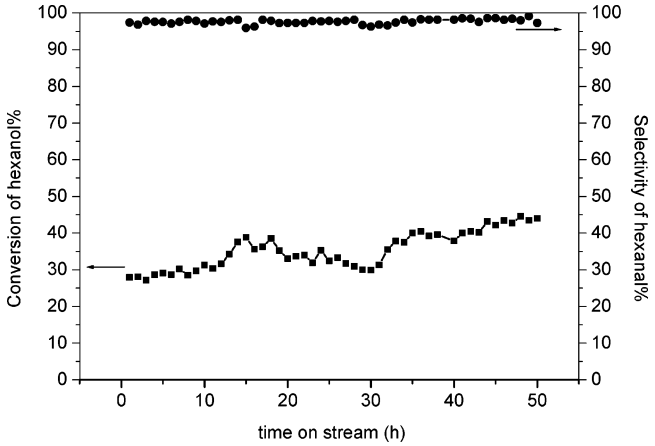

Figure 13. Stability of $Cu_2PMo_{11}VO_{40}$/MgO.

hexanal selectivity of 93.6%. It appears that the conversion of hexanol increases, whereas the selectivity of hexanal decreases with increase of temperature. The decrease in selectivity of hexanal is due to the formation of hexene and pentanal.

In the temperature region of ~513.2−593.2 K, the oxidative dehydrogenation of hexanol to hexanal is a main reaction, the yield of hexanal increases gradually with temperature. In the temperature range up to 573.2 K (even higher), a little (1.3%) of pentanal is observed, which indicates that the catalyst shows a higher oxidative dehydrogenation activity at higher temperature. On the other hand, in the temperature range of ~553.2−593.2 K, the catalytic reaction proceeds on both acid−base and redox centers of the catalyst surface. The product of hexanol dehydration proceeding on the acid−base sites is hexene; while the product of oxidative dehydrogenation of hexanol on redox sites is hexanal (or pentanal). Surprisingly, acidic sites are present under the catalytic conditions for the neutral salt ($Cu_2PMo_{11}VO_{40}$), although its activity is markedly low. Two explanations may be assumed: the acidity of neutral salt could be provided by dissociation of water molecule related to the metallic cation (or by formation of protons due to reduction of the metal ions)[41] or the acidic properties of this salt may come from the Lewis acidity.[31]

We have studied the variation of conversion and selectivities of this catalyst during 50 h at 553.2 K (Figure 13). During the first 10 h, a slight increase of the conversion and a stable selectivity for hexanal are observed. In the following 20 h, the conversion of hexanol increases then slightly decreases with time-on-stream but is higher than that in the initial 10 h. After 30 h, both conversion of hexanol and selectivity of hexanal are increased with time. The evolution of these catalytic properties can easily be explained by comparison to the IR spectra of the catalyst (Figure 9). For a sample tested at 553.2 K, the evolution of IR spectrum with running reaction shows an increase of the 1082.4-cm^{-1} signal. That a great change of the peak at 1082.4 cm^{-1} appears after reaction of 50 h can be assigned to split of the $P-O_a$ vibration. It is inferred that during the catalytic reaction the vanadium atoms unceasingly migrate from the Keggin unit producing a lacunary type structure. This state of the Keggin anion is highly reactive and can be the active species for the reaction.[42] Another possible assumption is removal of O^{2-} ions leading to the formation of a heteropolycompounds with oxygen vacancies during the reaction and the formation of the O^{2-} vacancies can improve the mobility of lattice oxygen necessary for a good catalyst for oxidative dehydrogenation process.[43]

4. Conclusions

Samples were prepared by impregnation method in ethanol solution, which does not hurt texture of the water sensitive MgO support and $Cu_2PMo_{11}VO_{40}$.

In the FTIR spectra of the fresh MgO-supported sample, the characteristic absorption peaks of the Keggin structure are very weak, which can be ascribed to a strong interaction between CPMV and support. The interaction may lead to partial degradation of the CPMV to form oligomerized polyoxometalate. However, the oligomers cannot exist for a long time but tend to degeneration and as a result monomers of the Keggin CPMV compound are obtained under the condition of heating (723.2 K) and gas phase selective oxidation (at 553.2 K for 50 h). Therefore, after thermal treatment and/or during catalytic reaction, the characteristic peaks of the Keggin structure become apparent.

After thermal treatment and under reaction condition, the vanadium ions migrate out of the Keggin anion to produce a lacunary structure. This state of the Keggin anion is highly reactive and can be the active state in catalytic reaction. In fact, the IR spectrum of the samples indicates that the catalyst after synthesis can form a lacunary structure, but the percentage of the part of vanadium ions migrated out of the Keggin anion is very low. After calcination at 723.2 K for 2 h or catalytic reaction at 553.2 K for 50 h, a great number of vanadium ions are in a tetrahedral environment outside the Keggin unit, i.e., a great number of lacunary structure is formed, which can be verified by the FTIR spectrum.

On the other hand, the lacunary Keggin anion is energetically more unstable and may also degenerate into the initial state of Keggin unit (Figure 8) at room temperature.

The EPR data imply the oxidation state of vanadium ion to be V^{5+} in the fresh-supported catalyst, which may autoreduce to V^{4+} due to the removal of the crystalline water, i.e., after the destruction of the secondary structure. In fact, during the catalytic reaction, a large number of V^{4+} ions are produced, which also probably accompanies reduction of Mo^{6+} to Mo^{5+}. The cation centers in the compound are reduced and become more oxygen-deficient than those in a lacunary structure, which enhances the formation of O^{2-} vacancies around the metal atoms. These oxygen vacancies are thus the basis for the cooperative action of oxygen in selective oxidation reactions. Furthermore, these oxygen-vacancies may also improve the reoxidative function of the catalyst. In that way, E. Blouet-Crusson[41] has proposed that a synergic effect between copper and vanadium clusters appears, which increases the mobility

of electrons and O^{2-} vacancies in to "bulk" (and surface) of catalyst during the catalytic reaction, and these small clusters (V, Cu) can also play a structural role and can also participate in the electronic and anionic transfers in the Keggin unit.

As illustrated in,[42] vanadium ions act as a stabilizing group keeping polyoxoanions at distances that hinder densification of the polyoxoanions and also as a linker for the polyoxometalates in their dehydrated state when oligomers form. Meanwhile, the lacunary species would form excellent ligands for vanadyl groups. In addition, vanadium ions may play a role of "electron reservoir".[44,45]

In conclusion, high activity and selectivity of $Cu_2PMo_{11}VO_{40}$/MgO catalyst for converting hexanol to hexanal are related to removal of vanadium from the Keggin unit after thermal treatment and gas phase selective oxidation to form lacunary species, and autoreduction of V^{5+} ions into V^{4+} ions. This behavior is correlated to high catalytic properties of this catalyst.

Acknowledgment. We thank the National Science Foundation (90306001) for the financial support of this investigation.

References and Notes

(1) Misono, M. *Catal. Rev. Sci. Eng.* **1987**, *29*, 269.
(2) Misono, M. *Catal. Rev. Sci. Eng.* **1988**, *30*, 339.
(3) Izumi, Y. *Catal. Today* **1997**, *33*, 371.
(4) Kim, J. S.; Kim, J. M.; Seo, G.; Park, N. C.; Niiyama, H. *Appl. Catal. A: Gen.* **1988**, *37*, 45.
(5) Mizuno, N.; Misono, M. *J. Mol. Catal.* **1994**, *86*, 319.
(6) Okuhara, J.; Mizuno, N.; Misono, M. *Adv. Catal.* **1996**, *41*, 113.
(7) Rabia, C.; Bettahar, M. M.; Fournier, M. *J. Chem. Phys.* **1997**, *94*, 1859.
(8) Bartoli, M. J.; Monceaux, L.; Bordor, E.; Hecquet, G.; Courtine, P. *Stud. Surf. Sci. Catal.* **1992**, *72*, 81.
(9) Akimoto, M.; Tsuchida, Y.; Sato, K.; Echigoya, E. *J. Catal.* **1981**, *72*, 83.
(10) Akimoto, M.; Shima, K.; Ikeda, H.; Echigoya, E. *J. Catal*. **1990**, *86*, 173.
(11) Marchal-Roch, C.; Bayer, R.; Moisan, J. F.; Teze, A.; Herve, G. *Top. Catal*. **1996**, *3*, 407.
(12) Bayer, R.; Marchal-Roch, C.; Liu, F. X.; Teze, A.; Herve, G. *J. Mol. Catal. A: Chem.* **1996**, *114*, 277.
(13) Aboukaïs, A.; Ghoussoub, D.; Blouet-Crusson, E.; Rigole, M.; Guelton, M. *Appl. Catal. A: Gen.* **1994**, *111*, 109.
(14) Deltcheff, C. R.; Aouissi, A.; Bettahar, M. M.; Launary, S.; Fournier, M. *J. Catal.* **1996**, *164* (1), 16.
(15) Fournier, M.; Thouvenot, R.; Rocchiccioli-Deltcheff, C. *J. Chem. Soc., Faraday Trans.* **1991**, *87*, 349.
(16) Peng, G.; Hu, C. W.; Wang, Y. H. *Chem. J. Chin. Univ.* **2000**, *23* (3), 478.
(17) Navalikhina, M. D.; Krylov, O. V. *Kinetics Catal.* **2001**, *42* (2), 264.
(18) Verboef, M. J.; Kooyman, P. J.; Peters J. A.; Bekkum, H. V. *Microporous Mesoporous Mater*. **1999**, *27* (2−3), 365.
(19) Vázquez, P. G.; Blanco, M. N.; Cáceres, C. V.*Catal. Lett.* **1999**, *60* (4), 205.
(20) Rires, A.; Payen, E.; Hubaut, R.; Vázquez, P.; Pizzio, L.; Cáceres, C.; Blanco, M. *Catal. Lett.* **2001**, *71* (3−4), 193.
(21) Wang, X. P.; Ye, X. K.; Wu, Y. *Chin. J. Catal.* **1996**, *17* (2), 149.
(22) Pron, A. *Synth. Met.* **1992**, *46* (3), 277.
(23) Hasik, M.; Turek, W.; Stochmal, E.; Lapkowski, M.; Pron, A. *J. Catal.* **1994**, *147* (2), 544.
(24) Hasik, M.; Proñ, A.; Pozniczek, J. Bielański, A.; Piwowarska, Z.; Kruczala, K.; Dziembaj, R. *J. Chem. Soc., Faraday Trans*. **1994**, *90* (14), 2099.
(25) Zhou, G. D.; Guo, X. H.; Liu , Y.; Bi, Y. L.; Zhen, K. J. *Chem. Resear. Chin. Univ*. **2001**, *17* (3), 293.
(26) Liu, S. X.; Li, Y. G.; Han, Z. B. *Chem. J. Chin. Univ.* **2002**, *23* (5), 277.
(27) Yadav, G. D.; Mistry, C. K. *J. Mol. Catal. A: Chem.* **2001**, *172* (1, 2), 135.
(28) Tsigdinos, A.; Hauada, C. J. *Inorg. Chem.* **1968**, *7*, 437.
(29) Tatibouët, J. M.; Montalescot, C.; Brückman, K. *Appl. Catal. A: Gen.* **1996**, *138*, L1.
(30) Cai, B. X. *Chem. J. Chin. Univ.* **1994**, *15* (11), 1690.
(31) Haber, J.; Pamin, K.; Matachowski, L.; Napruszewska, B.; Portowicz,J. *J. Catal*. **2002**, *207*, 296.
(32) Zhou, G. D.; Xu, Z. L.; Guo, X. H.; Zhuang, H.; Li, Y. N.; Lü, X. J.; Cheng, T. X.; Li, W. X.; Zhen, K. J. *React. Kinet. Catal. Lett.* **2005**, *85* (1), 57.
(33) Tsigdinos, G. A.; Halladal, C. J. *Inorg. Chem*. **1968**, *7* (3), 437.
(34) Ono, T.; Tanaka, Y.; Takeuchi, T.; Yamamoto, K. *J. Mol. Catal. A: Chem*. **2000**, *159*, 293.
(35) Knapp, C.; Ui, T.; Nagai, K.; Mizuno,N. *Catal. Today* **2001**, *71*, 111.
(36) Siahkali, A. G.; Philippou, A.; Dwyer, J.; Anderson, M. W. *Appl. Catal. A: Gen.* **2000**, *192*, 57.
(37) Kala Raj, N. K.; Deshpande, S. S.; Ingle, R. H.; Raja, T.; Manikandan, P. *Catal. Lett.* **2004**, *98* (4), 217.
(38) Kasztelan, S.; Payen, E.; Moffat, J. B. *J. Catal*. **1990**, *125*, 45.
(39) Mastikhin, V.; Kulikov, S.; Nosov, A.; Kozhevnikov, Y.; Mudrakovsky, Y.; Timofeeva, M. J. *Mol. Catal. A: Chem*. **1990**, *60*, 65.
(40) Lee, J. K.; Russo, V.; Melsheimer, J.; Köhler, K.; Schlögl, R. *Phys. Chem. Chem. Phys.* **2000**, *2*, 2977.
(41) Blouet-Crusson, E.; Rigole, M.; Fournier, M.; Aboukaïs, A.; Daubrege, F.; Hecquet, G.; Guelton, M. *Appl. Catal. A: Gen.* **1999**, *178*, 69.
(42) Lee, J. K.; Melsheimer, J.; Berndt, S.; Mestl, G.; Schlögl, R. *Appl. Catal. A: Gen.* **2001**, *214*, 125.
(43) Ernst, V.; Barbaux, Y.; Courtine, P. *Catal. Today* **1987**, *1*, 167.
(44) Akimoto, M.; Ikeda, H.; Okabe, A.; Echigoya, E. *J. Catal.* **1984**, *89*, 196.
(45) Otake, M.; Komiyama, Y.; Otaki, Y. *J. Phys. Chem*. **1973**, *77*, 2896.